Available online at www.sciencedirect.com
SCIENCE DIRECT®
Journal of Molecular Catalysis A: Chemical 208 (2004) 167–174
JOURNAL OF MOLECULAR CATALYSIS A: CHEMICAL
www.elsevier.com/locate/molcata

# Energetics of acrolein hydrogenation on Pt(1 1 1) and Ag(1 1 1) surfaces: a BOC-MP model study

B.C. Khanra [a,b,*], Y. Jugnet [a], J.C. Bertolini [a]

[a] *Institut de Recherches sur la Catalyse—CNRS, 2 Avenue Albert Einstein, F-69626 Villeurbanne, France*
[b] *Condensed Matter Physics Group, Saha Institute of Nuclear Physics, 1/AF Bidhannagar, Calcutta 700064, India*

Received 14 April 2003; accepted 30 June 2003

**Abstract**

Bond-order conservation-Morse potential (BOC-MP) model has been used to study the energetics of acrolein hydrogenation on Pt(1 1 1) and Ag(1 1 1) surfaces. For hydrogenation at low coverage of acrolein ($\theta = 1/9$), the model predicts an overall low activity for acrolein conversion and a lower selectivity for the formation of allyl alcohol. At higher acrolein coverage ($\theta = 1/4$), however, the total activity increases and the selectivity for the allyl alcohol is improved compared to its magnitude at low coverage. The results are in qualitative agreement with the experimental results on hydrogenation of similar α,β-unsaturated aldehyde on Pt surfaces indicating steric hindrance for the C=C bond hydrogenation at higher coverages. As for hydrogenation on Ag(1 1 1) surface, the energetics predict relatively higher selectivity for allyl alcohol compared to the selectivity on Pt(1 1 1) surface. The predictions are critically discussed with reference to the available experimental results.


*Keywords:* α,β-unsaturated aldehydes; BOC-MP model; DFT; Acrolein; Propanal

## 1. Introduction

The selective hydrogenation of α,β-unsaturated aldehydes to produce unsaturated alcohol is an important industrial catalytic process for manufacturing fine chemicals like perfumes, pharmaceuticals, and flavouring materials, etc. [1–3]. For these aldehydes, it is generally found that the hydrogenation of the C=C bond is faster than the hydrogenation of the C=O bond. In order to produce the unsaturated alcohol, however, the C=O bond needs to be selectively hydrogenated, while the hydrogenation of the olefinic C=C group, which produces saturated aldehyde, needs to be suppressed. It is a challenge for the catalysis chemists to find ways to increase the selectivity for the unsaturated alcohols with respect to the saturated aldehydes and understand the reaction mechanism.

From various experiments done on these α-unsaturated aldehydes [1–3], it has been found that various factors like the nature of supports, presence of electropositive species, poisons and reaction conditions, etc. may control the selectivity of the hydrogenation process. For example, it has been shown by Vannice and Sen [4] that Pt on $TiO_2$ reduced at 773 K hydrogenates C=O bond of crotonaldehyde more selectively compared to titania reduced at lower temperatures or other supports like silica or alumina. The higher activity for the C=O bond hydrogenation was attributed to the defect sites involving $Ti^{2+}$ or $Ti^{3+}$ species created at the metal-support interface at high reduction temperature or to oxygen vacancies. The presence of a second metal, more electropositive than the platinum group of metal catalysts, also helps to preferentially hydrogenate the C=O bond. For example, Fe in Pt has been shown to lead to higher production of unsaturated alcohols [5]. In some cases, improvements in selectivity have also been observed with increase in particle size [6,7]. This is particularly the case for the hydrogenation of larger molecules like methyl crotonaldehyde or cinnamaldehyde where the steric factor plays a role. Higher pressure of the unsaturated aldehydes also may cause steric hindrance to C=C bond hydrogenation [1,8].

To the best knowledge of the authors, no report investigating the mechanism of the hydrogenation reactions of these α,β-unsaturated aldehydes exists in literature. Model quantum chemical studies, carried out by Delbecq and Sautet [9–11] on the chemisorption of acrolein, crotonaldehyde and methyl crotonaldehyde on Pt and Pd surfaces, predict

* Corresponding author. Tel.: +91-33-23-37-53-45; fax: +91-33-23-37-46-37.
*E-mail address:* badal@cmp.saha.ernet.in (B.C. Khanra).

1381-1169/$ – see front matter © 2003 Elsevier B.V. All rights reserved.
doi:10.1016/S1381-1169(03)00507-7

qualitatively that inhibiting the C=C bond hydrogenation and enhancing the probability of C=O bond hydrogenation can be achieved by larger substituents like $CH_3$ or by using metals with larger radial spread of the d orbital like osmium and iridium. On Pt–Fe surface, Fe was shown [12] to promote the four-electron repulsion between the C=C bond and the Pt surface and enhances the C=O bond activation. Quantitative analysis predicting the activity and selectivity was beyond the scope of their work. This is because, a thorough understanding of the activity and selectivity would need a microkinetic analysis that takes into account all the reaction steps from the adsorption of the reactants to the desorption of the final products. However, due to the scarcity of required input data like the heats of adsorption of the molecules in all the intermediate states, their sticking coefficients and activation barriers for individual reaction steps, etc. a microkinetic analysis is not currently possible. We find that with available experimental and theoretical adsorption data on some of these molecules it is possible to study the energetics of the hydrogenation reaction and draw important conclusions. We have studied here the hydrogenation of acrolein, the smallest of the bifunctional unsaturated aldehydes, on Pt(1 1 1) and Ag(1 1 1) surfaces. This study has the potential of giving estimates of various activation barriers for the hydrogenation of the C=O bond giving allyl alcohol and hydrogenation of the C=C bond giving propanal, respectively. A comparison of these barriers and their dependence on coverages and the strengths of adsorption would then show the relative importance of the controlling parameters in the hydrogenation reaction. And it is the purpose of the present work to present the results of this analysis. The total reaction network is shown schematically in Fig. 1, and our current interest is in the reaction paths (A) and (B) showing C=C and C=O activation, respectively. Studies of the isomerisation reaction path from allyl alcohol to propanal [path (C)] and the paths leading to the final product propanol [(D) and (E)] are beyond the scope of the present work.

The model, used in this work is the bond-order conservation-Morse potential (BOC-MP) model [also known as unity bond index-quadratic exponential potential (UBI-QEP model)]. The model is well documented in literature [13–15] for its successful use in studying the energetics of reactions like Fischer–Tropsch synthesis, CO oxidation, NO reduction, methanol synthesis and ammonia synthesis, etc. In Section 2, we briefly discuss those aspects of the model that are relevant to this work. In Section 3, we present the results of our studies and discuss them thoroughly. The conclusions are drawn in Section 4.

## 2. The model

The basic principles of the bond-order conservation-Morse potential model are very simple as follows [13,14]:

(a) In a many body system like $M_n$–A ($n$ metal atoms and one adsorbate A), each two-body M–A interaction is described by a Morse potential

$$E[x(r)] = E_0[x^2(r) - 2x(r)] \quad (1)$$

where $x(r)$ is the bond-order defined by

$$x(r) = \exp\left\{-\frac{r - r_0}{a}\right\} \quad (a = \text{distance scaling constant}) \quad (2)$$

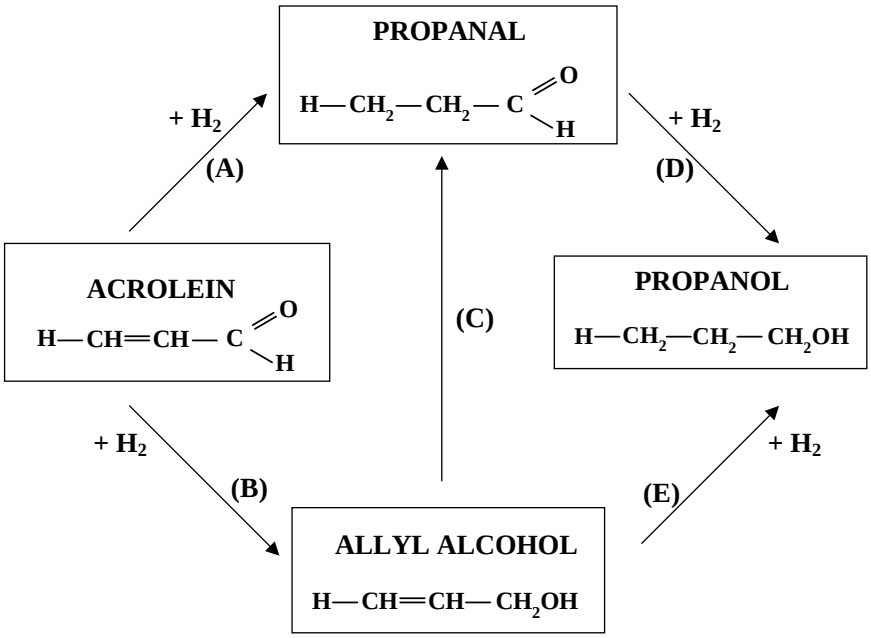


Fig. 1. Acrolein hydrogenation scheme.

and $E_0$ and $r_0$ are the equilibrium M–A bond energy and bond distance, respectively.

(b) The total bond energy for the $M_n$–A system is obtained by summation of the $n$ two-centre M–A interactions; and $n$ is limited to nearest neighbours only.

(c) The total bond-order is normalised to unity (or, bond-order is conserved)

$$X = \Sigma x_i = 1 \quad (i = 1, \ldots n). \tag{3}$$

The model rests on maximisation of total bond energies under the constraints of bond-order conservation. When applied to a diatomic molecule AB, the BOC-MP model can nicely correlate the heats of adsorption $Q_{AB}$ with the activation energy, $\Delta E^{d*}_{AB}$ for dissociation from a chemisorbed state through an expression [13]

$$\Delta E^{d*}_{AB} = \frac{1}{2}\left[D_{AB} + \frac{Q_A Q_B}{Q_{A+} Q_B} + Q_{AB} - Q_A - Q_B\right] \tag{4}$$

where $Q_{AB}$ and $D_{AB}$ are the heat of adsorption and the gas phase dissociation energy of the AB molecule, respectively. And assuming that for most cases of practical importance $\Delta E^{*}_{AB} \geq 0$, the activation barrier, $\Delta E^{r*}_{AB}$ for recombination of A and B from a chemisorbed state is given by BOC-MP model as [13]

$$\Delta E^{r*}_{AB} = \frac{1}{2}\left[Q_A + Q_B - Q_{AB} - D_{AB} + \frac{Q_A Q_B}{Q_{A+} Q_B}\right] \tag{5}$$

Essentially, the Eqs. (4) and (5) describe a form of linear relationship between the activation energies for dissociation and recombination with the heats of chemisorption. In fact, such linear relationships between activation barriers for dissociation and recombination with heats of adsorption were earlier shown to exist by Brønsted [16], and Evans and Polanyi [17] separately. In recent years, Pallassana and Neurock [18] and Nørskov et al. [19] have also shown that the Brønsted–Evans–Polanyi type relationship holds for ethylene hydrogenation and ammonia synthesis, respectively. The BOC-MP model, though ideal for reactions with small molecules like CO, NO, $O_2$ and $H_2$, may be applied to larger polyatomic molecules by partitioning the molecules as A and B sections. Some uncertainties and errors may enter in selecting the sections and in estimating the heats of adsorption of the molecular sections. However, in the absence of any better alternative model, the BOC model can indeed be used for reactions like acrolein hydrogenation on metal surfaces as demonstrated in this work.

In our studies of the energetics of acrolein hydrogenation, we have used the Eqs. (4) and (5) to estimate the activation barriers for the forward and reverse reaction, respectively. Since in the Arrhenius expression for the reaction rate equation

$$r = A \exp\left(-\frac{\Delta E}{RT}\right)$$

the activation barrier $\Delta E$ enters as an exponent, it controls the overall reaction rate. The role of the pre-exponential factor, $A$, is secondary. In the present case of acrolein hydrogenation, therefore, a comparative analysis of the various activation barrier heights has been made to show how the hydrogenation reaction is most likely to proceed step by step. This helped us to understand qualitatively the activity and selectivity of the Pt(1 1 1) and Ag(1 1 1) surfaces for the acrolein hydrogenation reaction.

## 3. Results and discussions

The most important factor that affects the accuracy of the BOC-MP analysis is the availability of accurate input data like the heats of adsorption of the molecules and their various fragments on the metal surfaces, and the gas phase dissociation energies. The best input data could be the data obtained from experiments like microcalorimetry, and temperature programmed desorption (TPD) for adsorption energies, and from spectroscopy for gas phase dissociation energies. The second best choice could be the data coming from molecular dynamics calculations or density functional calculations. The choice of our systems, namely, acrolein on Pt(1 1 1) and Ag(1 1 1) surfaces has been guided by this factor. For Pt(1 1 1) surface, the best data available to us are the adsorption data of Delbecq and Sautet [11] obtained from density functional theory (DFT). It was found that for higher coverage ($\theta = 1/4$) the di-$\sigma_{CC}$ was the most stable adsorption geometry followed by the $\eta_3$-*cis* geometry. On the other hand, for lower coverage ($\theta = 1/9$), $\eta_3$-*cis* ($\eta_4$-*trans*) was found to be the most stable geometry followed by the di-$\sigma_{CC}$ geometry. The geometries are shown schematically in Fig. 2. It is important to point out that irrespective of the *cis* or *trans* geometry in $\eta_3$ and $\eta_4$ coordination, the oxygen atom interacts directly with the metal atoms. We assume, therefore, that only these $\eta_3$ and $\eta_4$ coordinations

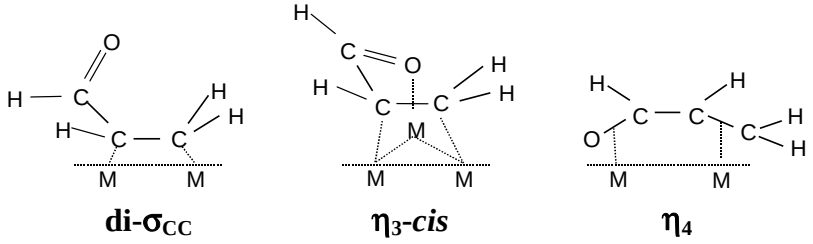


Fig. 2. Schematic geometries of adsorption of acrolein in di-$\sigma_{CC}$, $\eta_3$-*cis* and $\eta_4$ coordinations.

can preferentially hydrogenate the C=O bond leading to the production of allyl alcohol. On the other hand, in the di-$\sigma_{CC}$ adsorption geometry, only the C=C bond hydrogenation is assumed to take place leading to the selective production of saturated aldehyde (propanal). With the available DFT data, we were able to calculate the barriers for the hydrogenation of acrolein for both the allyl alcohol and propanal. We have ignored, for simplicity, the possibility of both C=C and C=O hydrogenation from the same $\eta_3$ or $\eta_4$ type bonding.

For acrolein hydrogenation on Ag(1 1 1) surface, we use the adsorption data from the work of Shustorovich [15] who, in turn, derived those data by applying the BOC-MP model to the experimental (TPD) results on acrolein/Ag(1 1 0) surface [20]. The input data for the acrolein/Ag(1 1 1) surface, thus, have an experimental basis. However, the data from Shustorovich's work help to follow the hydrogenation path to allyl alcohol only, as the data are available only for the $\eta_3$ adsorption geometry. For the di-$\sigma_{CC}$ geometry, we consider the adsorption data as variables, having values within ±10% of their values in the $\eta_3$ adsorption geometry. It will be shown that the activity and selectivity are not much sensitive to the heat of adsorption of acrolein or the products. The hydrogenation of acrolein to allyl alcohol via adsorption in the $\eta_3$ or $\eta_4$ geometry is a two-step process, where the addition of first hydrogen leads to the reaction intermediate allyl alkoxy; and the addition of the second hydrogen leads to the product, allyl alcohol. To describe this complete process, we would need four activation barriers, two for the forward reaction and two for the backward reaction. Similarly, for the hydrogenation of acrolein to propanal via the di-$\sigma_{CC}$ adsorption geometry, one needs four activation barriers. The scheme is shown in Table 1. In the column under activation barriers, the subscripts "1" and "2" denote the first and second reaction step, respectively; and the superscripts "f" and "r" denote the barrier for the forward and reverse reaction, respectively. The subscript "s" indicates that the species are adsorbed on the surface. The whole analysis rests on calculating these barriers from the Eqs. (4) and (5) and compare the two parallel reaction paths leading to allyl alcohol and propanal.

### 3.1. Reaction on Pt(1 1 1) surface

For reaction energetics on Pt(1 1 1) surface, we use the data as shown in Table 2 for two acrolein coverages, $\theta = 1/9$ and $\theta = 1/4$. Most of these data are taken from the DFT work of Delbecq and Sautet [11,21]. For acrolein and intermediates, we are considering the two adsorption configurations here, namely, $\eta_3$-*cis* and di-$\sigma_{CC}$ as they are energetically the most probable coordinations for chemisorption. For allyl alcohol and propanal, on the other hand, the DFT results show respectively the di-$\sigma_{CC}$ and O on-top as most stable configurations. For the 1/9 coverage, the DFT values are available for acrolein, the reaction intermediates and the hydrogenated products, allyl alcohol and propanal [11,21]. For the 1/4 coverage, however, the DFT data are available only for acrolein adsorption for the $\eta_3$-*cis* and di-$\sigma_{CC}$ coordinations. Therefore, for this 1/4 coverage we obtain the heats of intermediates and the products (allyl alcohol and propanal) from the 1/9 coverage values by considering the same percentage of change as for the heats of adsorption of acrolein at the two coverages. For hydrogen chemisorption energy on Pt(1 1 1) surface we take the value 61 kcals/mol [13,14]. For the gas phase total bond energies of the $C_3H_4O$, $C_3H_5O$ and $C_3H_6O$, we consider the values of 802, 816 and 918 kcals/mol, respectively [15,22]. The gas phase dissociation energies required for evaluating the activation barriers through Eqs. (4) and (5) are computed from these values. The energetics of acrolein hydrogenation on Pt(1 1 1) surface for 1/9 coverage would then be as shown in Fig. 3. The left half of the Fig. 3 shows the energetics of acrolein hydrogenation starting from adsorption in the $\eta_3$ coordination and hence the end product is allyl alcohol. The right half of the figure, on the other hand, shows the energetics for adsorption in the di-$\sigma_{CC}$ coordination. The arrows pointing outwards from the molecules indicate desorption with the energies shown. In absence of the data on desorption energy we show here the adsorption energy, assuming no activation barrier for adsorption. However, if there is activation energy for adsorption, then the heat of desorption, $E_d$, would be higher than the numbers shown. Therefore, the numbers indicate the lower limit of the heat of desorption. The arrows between the molecules indicate forward/reverse reactions with the corresponding activation barriers. Fig. 3 may be interpreted in the following way: in the $\eta_3$ coordination, the barrier for hydrogenation of acrolein to the reaction intermediate (allyl alkoxy) is $\Delta E_1^f = 11.24$ kcals/mol, which is much less than the energy for the acrolein molecule to

Table 1
Reaction steps and activation barriers

| Reaction | Geometry | Activation barriers |
|---|---|---|
| $CH_2CHCHO_s + H_s \leftrightarrow CH_2CHCH_2O_s$ | $\eta_3$ | $\Delta E_1^f, \Delta E_1^r$ |
| $CH_2CHCH_2O_s + H_s \leftrightarrow CH_2CHCH_2Oh_s$ | $\eta_3$ | $\Delta E_2^f, \Delta E_2^r$ |
| $CH_2CHCHO_s + H_s \leftrightarrow CH_3CHCHO_s$ | di-$\sigma_{CC}$ | $\Delta E_1^f, \Delta E_1^r$ |
| $CH_3CHCHO_s + H_s \leftrightarrow CH_3CH_2CHO$ | di-$\sigma_{CC}$ | $\Delta E_2^f, \Delta E_2^r$ |

Table 2
Heats of chemisorption ($Q$) of molecular species on Pt(1 1 1)

| Species | Coordination | $Q$ (kcals/mol) | |
|---|---|---|---|
| | | $\theta$ (1/9) | $\theta$ (1/4) |
| $CH_2CHCHO$ | $\eta_3$-*cis* | 24.3 | 20.8 |
| $CH_2CHCHO$ | di-$\sigma_{CC}$ | 22.5 | 23.2 |
| $CH_2CHCHOH$ | $\eta_3$-*cis* | 66.2[a] | 56.66[b] |
| $CH_3CHCHO$ | di-$\sigma_{CC}$ | 42.4[a] | 43.71[b] |
| $CH_2CHCH_2OH$ | di-$\sigma_{CC}$ | 25.5[a] | 21.83[b] |
| $CH_3CH_2CHO$ | O on-top | 6.0[a] | 6.19[b] |

[a] [21].
[b] Computed from the corresponding value for $\theta = 1/9$ keeping the same percentage change as was found for $Q$ of acrolein at the two coverages.

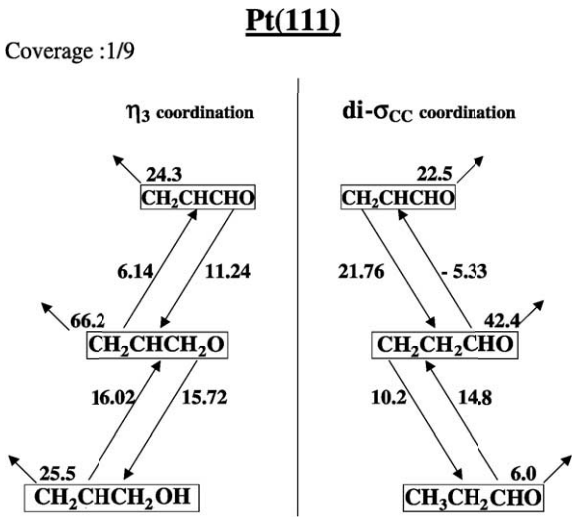


Fig. 3. Reaction energetics for acrolein hydrogenation on Pt(1 1 1) surface: coverage $\theta = 1/9$ (all energies in kcals/mol).

desorb ($E_d = 24.3$ kcals/mol). For the reaction intermediate, the barrier to dissociate into adsorbed acrolein and hydrogen (reverse reaction) is $\Delta E_1^r = 6.14$ kcals/mol, and therefore, much less than the barrier to further hydrogenation to allyl alcohol ($\Delta E_2^f = 15.72$ kcals/mol). The reaction intermediate, being in an adsorbed transition state, cannot desorb, as the barrier is prohibitively high ($E_d = 66.2$ kcals/mol). Finally, whatever little amount of allyl alcohol molecules are formed, the probability for them to dissociate into intermediate and hydrogen (reverse reaction) again is much higher than that to desorb from the surface. The barrier for the former is $\Delta E_2^r = 16.02$ kcals/mol compared to $E_d = 25.5$ kcals/mol for the latter. Thus, in essence, the acrolein molecules, once adsorbed in the $\eta_3$ coordination, have negligible chance to get desorbed.

A similar interpretation for hydrogenation with acrolein adsorbed in di-$\sigma_{CC}$ coordination would indicate that the barriers for the first hydrogenation to intermediate ($\Delta E_1^f = 21.76$ kcals/mol) and to desorption ($E_d = 22.5$ kcals/mol) are very close. That means a significant fraction of the molecules is desorbed on adsorption. Again, the barrier for hydrogenation from the reaction intermediate to propanal ($\Delta E_2^f = 10.2$ kcals/mol) is much higher than the barrier for dissociation (backward reaction) to acrolein and hydrogen ($\Delta E_1^r = -5.33$ kcals/mol). This would mean that the probability of propanal formation is highly reduced. However, once propanal is formed, it is likely to desorb, since the desorption barrier ($E_d = 6.0$ kcals/mol) is lower than the barrier for reverse reaction to go back to the intermediate ($\Delta E_2^r = 14.8$ kcals/mol) [it may be commented here that the negative values for activation energies, may not have a real meaning. For all practical purposes, these should be considered as zero].

Comparing the reaction energetics from the two adsorption geometries, shown in Fig. 3, it may then be concluded that:

(a) At acrolein coverage of 1/9, the total hydrogenation rate of acrolein on Pt(1 1 1) surface is small, as the number of both the desorbed allyl alcohol and propanal molecules, controlled by the respective activation barriers, would be less. We are keeping temperature out of consideration here, as the role of temperature would be partly governed by the Arrhenius equation.
(b) For the $\eta_3$ geometry, the highest barrier for obtaining the allyl alcohol is the desorption energy of allyl alcohol (25.5 kcals/mol); and this step may be the rate-limiting step in the hydrogenation to allyl alcohol. The rate-limiting step for the propanal formation is $\Delta E_1^f$ (21.76 kcals/mol).
(c) The difference between $E_d$ (allyl alcohol) and $\Delta E_2^r$ is 9.5 kcals/mol, which is high for the allyl alcohol to desorb. On the contrary, the difference between $E_d$ (propanal) and $\Delta E_2^r$ is $-8.8$ kcals/mol; which makes spontaneous desorption of propanal immediately after its formation possible.
(d) The selectivity would, thus, be higher for propanal formation compared to that for allyl alcohol.

Interestingly, the conclusions are in total agreement with what is found experimentally [1–3]. In other words, our energetics analysis shows for the first time why, in general, on pure Pt surfaces the hydrogenation of α,β-unsaturated aldehydes is slow; and why the selectivity is higher for saturated aldehydes than for the unsaturated alcohols.

For 1/4 coverage of acrolein, the results from energetics analysis are shown in Fig. 4. The following features may be noticed:

(a) Similar to the case of coverage 1/9, for 1/4 coverage the highest barrier to allyl alcohol formation is the desorption barrier of allyl alcohol ($E_d = 21.83$ kcals/mol).

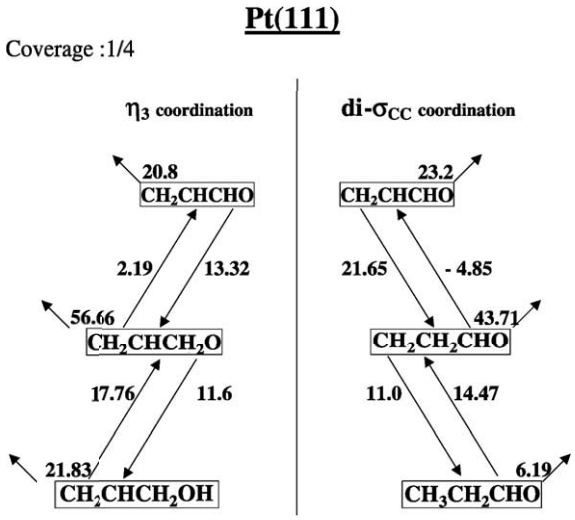


Fig. 4. Reaction energetics for acrolein hydrogenation on Pt(1 1 1) surface: coverage $\theta = 1/4$ (all energies in kcals/mol).

The highest barrier to propanal formation is $\Delta E_1^f$ (21.65 kcals/mol).

(b) Compared to 1/9 coverage, the desorption barrier of allyl alcohol is reduced by 3.67 kcals/mol; while the desorption barrier for propanal desorption has increased by 0.19 kcals/mol. This is a desirable effect in the hydrogenation to unsaturated alcohols.

(c) For 1/4 coverage, the difference between $E_d$ (allyl alcohol) and $\Delta E_2^r$ is 4.07 kcals/mol, much less compared to a value of 9.5 kcals/mol for 1/9 coverage. That means, the increase in coverage of acrolein has reduced this desorption barrier increasing the probability of allyl alcohol desorption. This is a much desired effect in the selective hydrogenation to unsaturated alcohols. On the contrary, the difference between $E_d$ (propanal) and $\Delta E_2^r$ is −8.28 kcals/mol, which is close to the difference of −8.8 kcals/mol for 1/9 coverage.

Summarising, the reaction rate at higher coverage of acrolein may be small. However, the increase in acrolein coverage may marginally improve the selectivity towards unsaturated alcohols. This is corroborated by the work of Birchem et al. [8] who have found in their experiment on hydrogenation of 3-methyl crotonlaldehyde at low pressure regime an increase in the selectivity to 3-methyl crotylalcohol with pressure.

### 3.2. Reaction on Ag(1 1 1) surface

For reaction on Ag(1 1 1) surface, we take the input data for the $\eta_3$ adsorption geometry from the work of Shustorovich [15], who obtained them by applying the BOC-MP model to the experimental data of Carter et al. [20] on Ag(1 1 0) surface. He calculated the intrinsic activation barriers for propylene oxidation and transformation of allyl alcohol and allyl chloride on clean and oxygen pre-dosed Ag(1 1 1) surface. For this, he needed to consider only the $\eta_2$ adsorption configuration of allylic species, which in the present study corresponds to the $\eta_3$ configuration. In our work, we had to consider also the di-$\sigma_{CC}$ geometry that may lead to formation of propanal. However, we do not have the experimental or theoretical values for the heats of adsorption of acrolein, the reaction intermediate or propanal on Ag(1 1 1) surface. Therefore, we keep them as variables and study their role on the activation barriers. For the heats of adsorption of acrolein and propanal in this geometry, we consider values 10% higher (or 10% lower) compared to the values in $\eta_3$ geometry. The input data are presented in Table 3. For the heat of adsorption of the reaction intermediate, we take a value of 40 kcals/mol—a value of the same order of magnitude as in the case of Pt(1 1 1) surface. For the heat of adsorption of hydrogen on Ag(1 1 1) surface, we take the value of 52 kcals/mol [13]. The energetics of acrolein hydrogenation would then be as shown in Fig. 5. It may be mentioned here that the activation barriers, shown on the left part of Fig. 5 were already calculated by Shustorovich [15] in connection with his work on allylic species, as discussed before. For the present work, in Fig. 5 the following important features are to be noticed:

Table 3
Heats of chemisorption ($Q$) of molecular species on Ag(1 1 1)

| Species | Coordination | $Q$ (kcals/mol) |
|---|---|---|
| $CH_2CHCHO$ | $\eta_3$-*cis* | 14.0 |
| $CH_2CHCHO$ | di-$\sigma_{CC}$ | 15.4 (*12.6*)[a] |
| $CH_2CHCH_2O$ | $\eta_3$-*cis* | 59 |
| $CH_2CH_2CHO$ | di-$\sigma_{CC}$ | 40[b] |
| $CH_2CHCH_2OH$ | $\eta_3$-*cis* | 14 |
| $CH_3CH_2CHO$ | di-$\sigma_{CC}$ | 15.4 (*12.6*)[a] |

[a] Taken 10% higher (the value in the parenthesis is 10% lower) than the corresponding value for $\eta_3$ geometry (see text).
[b] Taken close to the value on Pt(1 1 1) surface.

(a) The highest barrier in the $\eta_3$ geometry is $E_d$ (allyl alcohol) which is 14 kcals/mol. This is much lower than the corresponding $E_d$ (allyl alcohol) values from Pt(1 1 1) surfaces at both the coverages. Again, for the $\eta_3$ geometry, $\Delta E_1^f < \Delta E_1^r$ and $\Delta E_2^f < \Delta E_2^r$. Or, in other words, the barriers to forward reactions are much less compared to the barriers for reverse reactions. These relationships allow the hydrogenation reaction to proceed from adsorbed acrolein to allyl alcohol without losing much by the reverse reactions. Furthermore, $E_d$ (allyl alcohol) $< \Delta E_2^r$. All these conditions are favourable for higher selectivity to allyl alcohol.

(b) For the di-$\sigma_{CC}$ adsorption geometry, the highest barrier in the hydrogenation process is the desorption of propanal from the surface. The numbers shown outside the parenthesis are the barriers if the heat of adsorption of acrolein in the di-$\sigma_{CC}$ geometry is 10% higher than that for $\eta_3$ geometry; while the numbers in the parenthesis are the barriers if the heat of adsorption of acrolein in this geometry is 10% less than that for the $\eta_3$ geometry.

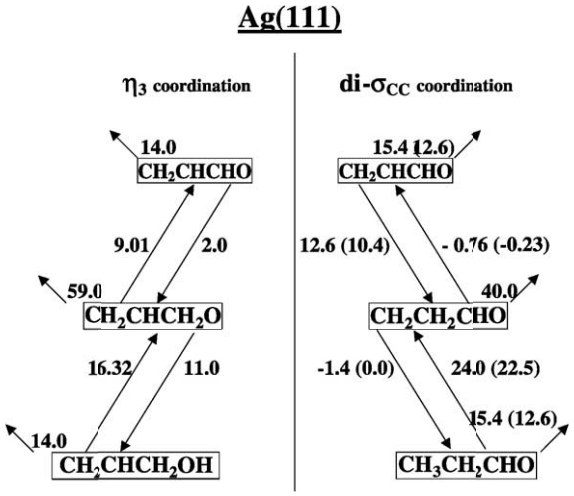


Fig. 5. Reaction energetics for acrolein hydrogenation on Ag(1 1 1) surface (all energies in kcals/mol).

It may be noticed that the variation in the magnitude of the barriers due to the variation of the heat of adsorption of acrolein or propanal is insignificant.

From a comparison of the two geometries, it may be concluded that on Ag(1 1 1) surface, both the parallel reactions are equally possible. The selectivity for both the products may be comparable.

On comparison with the results for acrolein hydrogenation on Pt(1 1 1) surfaces for low coverage (1/9) as well as for high coverage (1/4), the monometallic Ag(1 1 1) surface seems to be a better catalyst for selective hydrogenation of acrolein toward unsaturated alcohol. However, this is to be kept in mind that this energetics analysis deals only with the barriers to reaction from adsorbed acrolein and the reaction intermediates. The global selectivity would be governed also by the rate of adsorption and the sticking coefficients of the molecules on the surface which are not taken into consideration in this analysis. Experimentally, it was observed by Claus and co-workers [2,23,24] that monometallic silver catalyst were able to hydrogenate selectively the CO group of α,β-unsaturated aldehydes in the gas phase. They made an analysis of the selectivity results for crotonaldehyde hydrogenation on $Ag/SiO_2$ catalysts prepared by various techniques and found that the selectivity to crotyl alcohol on $Ag/SiO_2$-P was as high as 60%. The authors later switched to highly dispersed Au catalysts [25] to show their effectiveness in hydrogenating the C=O bond in comparison to supported Pt catalysts. In this respect, the present energetics analysis using BOC-MP model gives encouraging support to the possibility of using Ag and Au as catalysts for selective hydrogenation of α,β-unsaturated aldehydes. The method of preparation of the catalysts may hold the key to higher rate of adsorption, sticking probability and providing active centres for C=O bond hydrogenation.

## 4. Summary and conclusions

Hydrogenations of α,β-unsaturated aldehydes on transition metals involve several elementary steps. A thorough understanding of the activity and selectivity of the catalysts for the hydrogenation reactions would need a comprehensive knowledge about the activation barriers for these elementary steps. The BOC-MP model has been used to estimate these barriers for acrolein hydrogenation on Pt(1 1 1) and Ag(1 1 1) surfaces. This led us, for the first time, to understand the reactions better from their energetics. We have assumed that $\eta_3$ coordination leads to C=O activation producing allyl alcohol and di-$\sigma_{CC}$ coordination activates C=C bond producing propanal. Under these assumptions, the energetics analysis has shown that:

(a) The overall activity of Pt(1 1 1) surface can be small for the hydrogenation of acrolein. This means the total conversion of acrolein to allyl alcohol and propanal would be small.
(b) The selectivity for allyl alcohol marginally increases with acrolein coverage on Pt(1 1 1) surface.
(c) And on Ag(1 1 1) surface, the selectivity to allyl alcohol may be higher than that on Pt(1 1 1) surface.

The barriers for the elementary steps, however, cannot be obtained from experiments, as from experiments one can estimate only one global activation barrier. But from the magnitude of all the barriers one can comment on the global reaction rate and the selectivity, as has been done in this work.

Regarding the adsorption configurations on platinum, there is some experimental evidence to show hydrogenation in the $\eta_4$ geometry where both the C=C and C=O bonds may be activated [2,26]. However, the DFT calculations [11] at acrolein coverages of 1/4 and 1/9 show higher stability for $\eta_3$ and di-$\sigma_{CC}$ geometries and not for $\eta_4$ geometry. Therefore, in the present work, which rested on the DFT results, only the $\eta_3$ and di-$\sigma_{CC}$ geometries have been considered.

The accuracy of the predictions of the BOC-MP model depends on the accuracy of the input data. In this work, we had the data from DFT calculations, some from experiments and some are obtained from approximations. Lastly, availability of accurate experimental/theoretical data in future would help us to have a better understanding of the hydrogenation process of not only acrolein but also of larger molecules like crotonaldehyde, methyl-crotonaldehyde and cinnamaldehyde, etc.

## Acknowledgements

The authors thank Drs. F. Delbecq, D. Loffreda and P. Sautet for providing them the data on heats of adsorption of reaction intermediates and final products before their publication. One of the authors (BCK) acknowledges CNRS for supporting his stay at IRC as associate researcher.

## References

[1] P. Gallezot, D. Richard, Catal. Rev. Sci. Instrum. 40 (1998) 81.
[2] P. Claus, Top. Catal. 5 (1998) 51.
[3] V. Ponec, Appl. Catal. A: Gen. 149 (1997) 27.
[4] M.A. Vannice, B. Sen, J. Catal. 115 (1989) 65.
[5] P. Beccat, J.C. Bertolini, Y. Gauthier, J. Massardier, P. Ruiz, J. Catal. 126 (1990) 451.
[6] A. Giroir-Fendler, D. Richards, P. Gallezot, Catal. Lett. 5 (1990) 175.
[7] Y. Nitta, K. Ueno, T. Imanaka, Appl. Catal. 56 (1989) 9.
[8] T. Birchem, C.M. Pradier, Y. Berthier, G. Cordier, J. Catal. 146 (1994) 503.
[9] F. Delbecq, P. Sautet, J. Catal. 152 (1995) 217.
[10] F. Delbecq, P. Sautet, J. Catal. 164 (1996) 152.
[11] F. Delbecq, P. Sautet, J. Catal. 211 (2002) 398.
[12] R. Hirschl, F. Delbecq, P. Sautet, J. Hafner, J. Catal. 217 (2003) 354.
[13] E. Shustorovich, Adv. Catal. 37 (1990) 101.
[14] E. Shustorovich, H. Sellers, Surf. Sci. Rep. 31 (1998) 1.
[15] E. Shustorovich, Surf. Sci. 279 (1992) 355.
[16] N. Brønsted, Chem. Rev. 5 (1928) 231.

[17] M.G. Evans, N.P. Polanyi, Trans. Faraday Soc. 34 (1938) 11.
[18] V. Pallassana, M. Neurock, J. Catal. 191 (2000) 301.
[19] J.K. Nørskov, T. Bligaard, A. Logadottir, S. Bahn, L.B. Hansen, M. Bollinger, H. Bengaard, B. Hammer, Z. Sljivancanin, M. Mavrikakis, Y. Xu, S. Dahl, C.J.H. Jacobsen, J. Catal. 209 (2002) 275.
[20] R.N. Carter, A.B. Anton, G. Apai, Surf. Sci. 290 (1993) 319.
[21] F. Delbecq, P. Sautet, private communication.
[22] D.R. Lide (Ed.), Handbook of Chemistry and Physics, vol. 9, CRC Press, Boca Raton, 1994, pp. 51–73.
[23] P. Claus, P. Kraak, R. Schödel, in: H.U. Blaser, A. Baiker, R. Prins (Eds.), Studies in Surface Science and Catalysis, Heterogeneous Catalysis and Fine Chemicals, vol. 108, fourth ed., Elsevier, Amsterdam, 1997, p. 281.
[24] P. Claus, H. Hofmeister, J. Phys. Chem. B 103 (1999) 2766.
[25] P. Claus, A. Brückner, C. Mohr, H. Hofmeister, J. Am. Chem. Soc. 122 (2000) 11430.
[26] H. Yoshitake, Y. Iwasawa, J. Chem. Soc. Faraday Trans. 88 (1992) 503.